 doi:10.20944/preprints202009.0365.v1

Article

Gray- and Black-Box Modeling of Ships and Wave Energy Converters Based on Bayesian Regression

Yanjun Liu [1,2,3], Yifan Xue [2,3,*], Shuting Huang [2,3,*], Qianfeng Jing [4] and Gang Xue [2,3]

[1] School of Mechanical Engineering, Key Laboratory of High Efficiency and Clean Mechanical Manufacture, Shandong University, Jinan 250061, China; lyj111ky@163.com

[2] Institute of Marine Science and Technology, Shandong University, Qingdao 266237, China; xuegangzb@163.com

[3] Laboratory for Marine Geology Qingdao National Laboratory for Marine Science and Technology; Qingdao 266200, China

[4] Navigation College, Dalian Maritime University, Dalian 116026, China; jdf@dlmu.edu.cn

* Correspondence: xueyifan@mail.sdu.edu.cn; (Y.X.); hst@sdu.edu.cn; (H.S.)

Abstract: Establishing an accurate mathematical model is the foundation of simulating the motion of marine vehicles and structures, and it is the basis of modeling-based control design. System identification from observed input-output data is a practical and powerful method. However, for modeling objects with different characteristics and known information, a single modeling framework can hardly meet the requirements of model establishment. Moreover, there are some challenges in system identification, such as parameter drift and overfitting. In this work, three robust methods are proposed for generating ocean hydrodynamic models based on Bayesian regression. Two Bayesian techniques, semi-conjugate linear regression and noisy input Gaussian process regression, are used for parametric and nonparametric gray-box modeling and black-box modeling. The experimental free-running tests of the KVLCC2 ship model and a multi-freedom wave energy converter (WEC) are used to validate the proposed Bayesian models. The results demonstrate that the proposed schemes for system identification of the ship and WEC have good generalization ability and robustness. Finally, the developed modeling methods are evaluated considering the aspects required conditions, operating characteristics and prediction accuracy.

Keywords: System identification; Hydrodynamic model; Ship maneuvering; Wave energy converter; Bayesian regression

1. Introduction

A mathematical model is an approximate description of a physical system, and they are the foundation of designing, simulation and control. Establishing an accurate and practical hydrodynamic model has always been a research hotspot in the field of ocean engineering. For ships, the high precision of ship maneuvering systems plays a crucial role in ship controller design and operation [1]. A wave energy converter (WEC) needs an active control strategy to maximize its efficiency in a wide range of operating conditions [2]. Various methods have been proposed to construct the hydrodynamic model in naval architecture.

Depending on whether prior knowledge and physical laws are used in modeling, the modeling methods can be categorized as white-box modeling, gray-box modeling and black-box modeling methods [3]. White-box modeling is the case in which a model is perfectly known. It needs to predefine the mathematical structure entirely from prior knowledge and physical insight. However, due to the strong nonlinearity of water resistance and the randomness of turbulence [4], it is extremely difficult to establish an accurate white-box model of a marine vehicle or structure. The practical way is to first select the model through certain criteria, and then estimate the parameters in the selected model from observation data with system identification. This modeling method is called gray-box modeling. Specific to marine equipment, the most commonly used approach is to establish

 doi:10.20944/preprints202009.0365.v1

the equation according to Newton's second law and then substitute the fitted regression hydrodynamic force in it.

The traditional way to fit the hydrodynamic force in gray-box model is to expand it into a linear function of velocity. For ship modeling, different parametric model structures, such as Abkowtiz model [5,6], MMG model [7] and Nomoto model [8], have been proposed and validated over the years. The hydrodynamic parameters can be obtained by a captive model test with planar motion mechanism (PMM), computational fluid dynamics (CFD) and free-running tests with system identification [9]. Among the above approaches, the system identification with free-running test has been proven to be a powerful and practical method with lower experiment cost [10]. System identification is a general term for estimating parameters from observed input and output data, which provides a reliable mathematical surrogate model in multiple engineering areas [11]. The least square (LS) [12], extended Kalman filter (EKF) [13] and maximum likelihood (ML) [14] algorithms are introduced to identify the hydrodynamic derivatives and proved the effectiveness. Over the last decade, some new methods, with stronger generalization ability and robustness, based on machine learning have also been applied to the estimation of hydrodynamic parameters. Minimizing the Hausdorff metric with the genetic algorithm (GA) can alleviate the impact of noise-induced problems [10]. Mei et al. [15] introduced model reference and random forest (RM-RF) to model ship dynamic model and validated the proposed scheme with free-running test data. Wang et al. [16] presented nu-Support Vector Machine (v-SVM) to improve the robustness of the algorithm.

In the gray-box modeling of wave energy community, Cummin's equation [17] is used to define the hydrodynamic model. Generally, there are two ways to determine the equation. Typically, the hydrodynamic model is predefined as the linear model and solved by the potential flow theory [18], whereby the problem is simplified and linearized through assumptions of small amplitude oscillations. However, the simplified linearizing assumptions are invalid when the WECs have large amplitude motions resulting from energetic waves or sustained wave resonance [19]. An alternative method is to use system identification. The training data can be obtained from CFD simulation [2] or scale experiments in a towing tank [20,21]. A popular method is to estimate the real hydrodynamic force using an EKF observer, which assumes that the excitation force can be represented as the sum of a finite set of harmonic components [22,23].

The gray-box modeling methods mentioned above are all parameterized. Recently, a nonparametric gray-box model has been put forward in some studies, and encouraging results have been obtained. The model still follows the framework of Newton's law, and the force element, which is difficult to determine, is directly replaced by a machine learning model of related variables. Wang et al. [24] used SVM to replace the Taylor expansion in Abkowtiz model, and they compared the accuracy and computation speed with parametric gray-box and black-box modeling. Xu and Guedes Soares [25] proposed a nonlinear implicit model with nonlinear kernel-based Least Square SVM for a maneuvering simulation of a container ship in shallow water. The forces and moments in [25] are obtained by a PMM test and then trained as outputs for an SVM model related to speed and water depth. In the study of WEC [26], an observer-based unknown input estimator is used to estimate the wave excitation force, then a Gaussian Process (GP) is adopted to forecast the wave excitation force. On the one hand, the nonparametric gray-box model directly substitutes the information of the object itself. On the other hand, compared with linear expansion, it can better fit the hydrodynamic force. Therefore, this method is worth studying and comparing with the experimental data of more devices.

Recently, Bayesian regression has been successful applied in multiple fields for parameter estimation and black-box modeling. Bayesian methods have significant advantages in modeling with good statistical properties, predictions for missing data and forecasting [35-37]. Moreover, Bayes' rule offers a reasonable way to update beliefs in light of training data, and the hyperparameters in the Bayesian scheme have an intuitive meaning [38]. Bayesian regression models can work well in dynamic system modeling with a relatively small number of training data points and noisy output [39]. With regards to parametric gray-box modeling, ship dynamic models based on conjugate and semi-conjugate Bayesian regression (ScBR) are adopted to estimate the hydrodynamic parameters [40]. For the black-box modeling, Ariza Ramirez et al. [32] used multioutput GPs to identify the ship

Preprints (www.preprints.org) | NOT PEER-REVIEWED | Posted: 16 September 2020 doi:10.20944/preprints202009.0365.v1

dynamic system, and showed that the GP scheme has better generalization than RNN. Astfalck et al. [41] used a series of Bayesian methods to quantify the extremal responses of a floating production storage and offloading (FPSO) vessel. GP introduces a complexity penalty and it has an automatic regularization built into it through its foundation in Bayesian probability theory. The advantage of the complexity penalty is that, unlike other methods such as neural networks, Gaussian process regression has a far smaller risk of overfitting. However, the Bayesian approaches for gray-box and black-box modeling of marine dynamic model has not been investigated and compared considering the aspects of prerequisite conditions, accuracy and robustness under experimental data.

This article contributes to the use of Bayesian regression to identify the nonlinear dynamic model of a container ship and an oscillating buoy WEC with gray-box modeling and black-box modeling. First, the Bayesian regression algorithms, including semi-conjugate regression (ScBR) and noisy input Gaussian process (NIGP), are introduced. Then, the parametric, nonparametric gray-box modeling and black-box modeling schemes based on Bayesian algorithms are proposed for the ship and WEC respectively. These proposed schemes are validated and compared using experimental data. Finally, the capabilities and challenges of the proposed models are further discussed.

This paper is organized as follows. Section 2 describes the marine dynamic model. The algorithms of ScBR and NIGP are depicted in Section 3. In Sections 4 and 5, the identification schemes of the ship and WEC and experimental examples are presented to demonstrate the distinction and effectiveness of the proposed two methods. Section 6 presents the main conclusions and a further discussion.

2. Kinematic model

The classical kinematic model in naval architecture is motivated by Newton's second law, and the rigid-body kinematics equations can be expressed in vector form as [42]

$$\begin{gathered} \mathrm{M}_{RB}\dot{\mathcal{V}} = \tau_{RB} - C_{RB}(\mathcal{V}) \\ \tau_{RB} = \tau_h + \tau_{env} + \tau_{control} \end{gathered} \tag{1}$$

where M_{RB} is the rigid-body inertia matrix; $C_{RB}(\mathcal{V})$ is a matrix of rigid-body Coriolis and centripetal terms; τ_{RB} is a vector of generalized forces containing hydrodynamic waver resistance, τ_h, environmental forces, τ_{env}, and control forces, $\tau_{control}$. $\mathcal{V}$ denotes the generalized velocity in 6 (degree of freedom) DOF, the notation of motion variables is shown in Table 1.

Table 1. Notation of motion variables

DOF	Motions	Forces	Linear velocity	Positions
1	Surge	F_1	u	x
2	Sway	F_2	v	y
3	Heave	F_3	w	z
	Rotations	**Moments**	**Angular velocity**	**Rotation angles**
4	Roll	M_1	p	φ
5	Pitch	M_2	q	θ
6	Yaw	M_3	r	ψ

The marine dynamic model is essentially a nonlinear autoregressive model with an exogenous input (NARX) system, and the predictions are based on the previous measurements of the input signals and output signals [39]. Fig. 1 shows the NARX configuration for dynamic system, where c_k denotes the command signals such as propeller speed and rudder angle of the ship (Ariza Ramirez et al., 2018); y_k is the original output; $\hat{y}_k$ is polluted by noise, ϵ; z stands for the z-transformation; and subscript k denotes time step.

 doi:10.20944/preprints202009.0365.v1

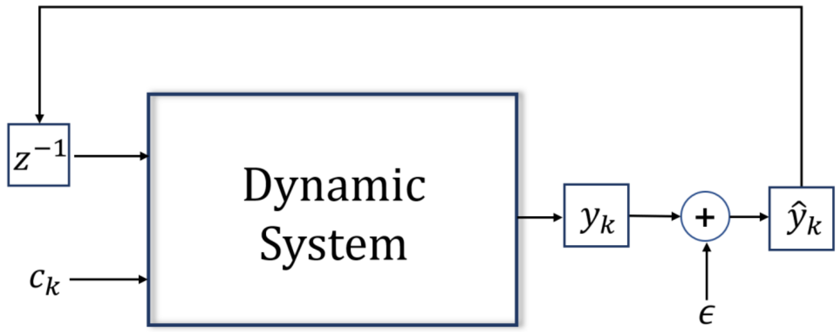

Figure 1. NARX model

3. Bayesian regression framework

3.1. Simi-conjugate Bayesian regression

The object of linear regression is to estimate the hydrodynamic parameters β in damping matrix τ_h, the form of multiple linear regression as

$$y_t = x_t\beta + \varepsilon_t \tag{2}$$

where t=1,…n denotes time; y_t is the observed response; x_t is a $1 \times c$ row vector of the observed values of c predictors; β is a $c \times 1$ column vector of regression parameters corresponding to the variables that consist of the columns of x_t; and ε_t is the random disturbance that has a mean of zero and common variance of σ^2.

Bayes theorem treats β and σ^2 as random variables belonging to some probability distributions. Generally, the Bayesian analysis process updates the probability density function (PDF) of the parameters by incorporating information about the parameters from the training data. Bayes' theorem gives the posterior PDF as

$$P(parameters|data) = \frac{P(data|para)P(para)}{P(data)} \tag{3}$$

According to the central limit theorem, most of the measured value distributions can be approximated by a normal distribution or a Gaussian distribution. A popular choice is the normal-inverse-gamma conjugate model [43], in which β obeys the multivariate normal distribution ($\mathcal{N}$) and σ^2 is the inverse gamma (IG) distribution. Equation (3) can be abbreviated as follows:

$$\pi(\beta, \sigma^2|y, x) \propto \mathcal{N}(\beta)\mathcal{N}(\sigma^2)\prod_{t=1}^{n}\phi(y_t; x_t\beta, \sigma^2) \tag{4}$$

where $\phi(y_t; x_t\beta, \sigma^2)$ is the Gaussian probability density with mean $x_t\beta$ and variance σ^2 on y_t. The regression model is divided into conjugate and semi-conjugate Bayesian regression depending on whether the parameters and disturbance are independent.

In practical engineering applications, parameters and noise are often not independent of each other [44]. The prior distributions of β and σ^2 are as follows when β and σ^2 are dependent:

$$\begin{gathered} \beta \ |\sigma^2 \sim N_c(\mu, V) \\ \sigma^2 \sim IG(A, B) \end{gathered} \tag{5}$$

where μ is the mean value ($c \times 1$ vector), V is the $c \times c$ diagonal matrix in which each element equals the prior variance factor of β_j, and $IG(A, B)$ denotes the inverse gamma distribution with shape A and scale B.

The conditional posterior distribution of β and σ^2 can be obtained:

$$\beta|\sigma^2, y, x \sim N_c((V^{-1} + \sigma^{-2}X^TX)^{-1}[\sigma^{-2}(X^TX)\hat{\beta} + V^{-1}\mu], (V^{-1} + X^TX)^{-1}) \tag{6}$$

$$\sigma^2|\beta, y, x \sim IG(A + \frac{n}{2}, (B^{-1} + \frac{1}{2}SSR(\beta))^{-1}) \tag{7}$$

Preprints (www.preprints.org) | NOT PEER-REVIEWED | Posted: 16 September 2020 doi:10.20944/preprints202009.0365.v1

where X is an $n \times c$ matrix of training data and $SSR(\beta)$ is given by

$$SSR(\beta) = \sum_{i=1}^{n} (y_i - \beta^T x_i)^2 = (y - X\beta)^T (y - X\beta) \tag{8}$$

Since β and σ^2 are mutually influential, their posterior distributions are not analytically tractable. Some numerical integration techniques based on the Markov chain Monte Carlo method have been proposed to solve this problem. In the present work, the Gibbs sampler [45] is applied to approximate the posterior of β and σ^2. The Gibbs sampler is an iterative algorithm that constructs a dependent sequence of parameter values whose distribution converges to the target joint posterior distribution. The values of parameters are the mean of the posterior of β.

In multivariate linear regression, introducing the L_2-norm into the algorithm to overcome the problems of multicollinearity and overfitting is a general accepted and effective method, such as ridge regression. ScBR naturally introduces the norm through prior parameters. These type of parameters in the algorithm framework are called hyperparameters in machine learning. Compared to other algorithms, the hyperparameters of the prior distribution, such as the mean and variance, in the Bayesian approach have a clear and intuitive meaning: The value of the prior mean μ represents the parameter to be identified, which we subjectively set before the regression is performed. When there is no other prior information about the parameter to be estimated, the mean μ is usually set to zero. The prior variance is obtained by Bayesian optimization algorithm (BOA). BOA is a powerful global optimization algorithm, which is usually used in the hyperparameter optimization of machine learning in cases with fewer hyperparameters and slower operations of the objective model [46]. More details about the ScBR with BOA can be found in our previous work [40].

3.2. Noisy input Gaussian process

GP can be viewed as a collection of random variables with a joint Gaussian distribution for any finite subject. GP can be conveniently specified by a mean function, $m(x)$, and a covariance function, $k(x, x')$, as

$$m(x) = E[f(x)] \tag{9}$$

$$k(x, x') = E[(f(x) - m(x))(f(x') - m(x'))] \tag{10}$$

where E denotes the expectation operator.

GP regression approximates an unknown function, $f(x)$, which maps a D-dimensional input to a scalar output value, f. A number of training points n, which include c-dimensional inputs, $\{x_t\}_{t=1}^{n}$ and noisy observations $\{y_t\}_{t=1}^{N}$ are given. These collections of variables are denoted as the $n \times c$ input, X, and the $n \times 1$ output vector, y. The regular Gaussian process (RGP) assumes that the training outputs are corrupted by noise,

$$y = f(x) + \epsilon_y \tag{11}$$

where ϵ_y is Gaussian white noise with zero mean and variance ${\sigma_y}^2$. The regular GP regression defines a GP prior on the function values,

$$p(f|X) = \mathcal{N}(m(X), k(X, X)) \tag{12}$$

With these modeling assumptions in place, the likelihood function can be obtained,

$$p(y|f, X) = \prod_{t=1}^{n} \mathcal{N}(y_t; f_t, {\sigma_y}^2) \tag{13}$$

Then, combining the prior Equation (12) and the likelihood function Equation (13), we can obtain the posterior probability distribution and predict the function values, f^*, at a whole set of test points X^*.

$$\begin{bmatrix} f^* \\ y \end{bmatrix} \sim \mathcal{N}\left(\begin{bmatrix} m(X^*) \\ m(X) \end{bmatrix}, \begin{bmatrix} K(X^*, X^*) & K(X^*, X) \\ K(X, X^*) & K + {\sigma_y}^2 I \end{bmatrix}\right) \tag{14}$$

which leads to the RGP regression predictive equations,

$$p(f^*|X^*, X, y) = \mathcal{N}(m, s) \tag{15}$$

$$m = m(X^*) + K(X^*, X)[K(X, X) + \sigma_y{}^2 I]^{-1}(y - m(X)) \tag{16}$$

$$s = k(X^*, X^*) - K(X^*, X)[K(X, X) + \sigma_y{}^2 I]^{-1} K(X, X^*) \tag{17}$$

The traditional formulation of GP regression only considers output noise $\sigma_y{}^2$, while the input data are assumed to be noise-free. However, the noise in the output will be passed to the input in the NARX models, as shown in Fig. 1. McHutchon and Rasmussen proposed the NIGP method which does take into account the input noise and posterior data [47]. NIGP further assumes that the inputs are also noisy, and the actual inputs and outputs are labeled $\tilde{x}$ and $\tilde{y}$, respectively.

$$x = \tilde{x} + \epsilon_x \tag{18}$$

where ϵ_x is Gaussian white noise with zero mean and variance $\sum_x$. The prerequisites for this model are that each input dimension is independently corrupted by noise, so $\sum_x$ is diagonal. Similar to Equation (11), the output function can be written as:

$$y = f(\tilde{x} + \epsilon_x) + \epsilon_y \tag{19}$$

We can use a first order Taylor series expansion of the GP latent function, f, to write an approximation to Equation (19) as,

$$y = f(x) + \epsilon_x^T \frac{\partial f(\tilde{x})}{\partial \tilde{x}} + \epsilon_y \tag{20}$$

Note that the expansion can be expanded to higher terms. However, these higher term calculations are computationally costly and provide no significant improvement. For notational convenience, the derivative of one GP mean function in Equation (20) will be denoted as $\partial_{\bar{f}}$, a c-dimensional vector. $\triangle_{\bar{f}}$, an $n \times c$ matrix, denotes the value of the derivative for the n functions. Given that the GP prior is the same as that of the RGP, $p(f|X) = \mathcal{N}(0, K(X, X))$, where $K(X, X)$ is the $n \times n$ training data covariance matrix, we can obtain the predictive posterior mean and variance as

$$\mathbb{E}[f^*|X, y, X^*] = K(X^*, X)\,[K(X, X) + \sigma_y{}^2 I + diag\{\triangle_{\bar{f}} \textstyle\sum_x \triangle_{\bar{f}}^T\}]^{-1} y \tag{21}$$

$$\mathbb{V}[f^*|X, y, X^*] = k(X^*, X^*) - K(X^*, X)\,[K(X, X) + \sigma_y{}^2 I + diag\{\triangle_{\bar{f}} \textstyle\sum_x \triangle_{\bar{f}}^T\}]^{-1} K(X, X^*) \tag{22}$$

where the notation "*diag*" results in a diagonal matrix.

In this way, the input is treated as deterministic and a correction term, $diag\{\triangle_{\bar{f}} \sum_x \triangle_{\bar{f}}^T\}$, is added to the output noise. More specifically, the influence of the input noise depends on the slope of the function we are approximating. Our model is essentially same as an RGP if the posterior mean is fully flat. The next problem is how to approximate the posterior distribution based on its derivative.

Compared to the RGP, the NIGP introduces extra hyperparameters ϵ_x per input dimension. A major advantage of this model is that these hyperparameters can be trained alongside any others by ML. The marginal likelihood function of the NIGP is,

$$-log \;\; p_{NIGP}(y|X, \theta) = \frac{1}{2}\log|K_n| + \frac{1}{2}(m(X) - y)^T \mathcal{B} + \frac{N}{2} log 2\pi \tag{23}$$

where,

$$K_n = K(X, X) + diag\{\triangle_{\bar{f}} \textstyle\sum_x \triangle_{\bar{f}}^T\} + \sigma_y{}^2 I \tag{24}$$

$$\mathcal{B} = K_n{}^{-1}(m(X) - y) \tag{25}$$

The solution to estimating the hyperparameters is a two-step approach. First, we evaluate a regular GP without any input noise. Then, we calculate the derivatives and use them to approximate the posterior distribution. The marginal likelihood of the GP with corrected variance is then computed. We can cycle this process until the convergence; this step involves chaining the derivatives of the

Preprints (www.preprints.org) | NOT PEER-REVIEWED | Posted: 16 September 2020 doi:10.20944/preprints202009.0365.v1

marginal likelihood back through the slope calculation. Moreover, the gradient descent algorithm is employed to tune the hyperparameters. A complete explanation can be found in [48] and some supplementary notes are in Bijl's study [49].
The proposed model adopts the commonly used squared exponential (SE) covariance function expressed as

$$k(x_i, x_j) = \sigma_f{}^2 \exp(-\frac{1}{2}(x_i - x_j)^T \Lambda (x_i - x_j) \quad (26)$$

where σ_f denotes the amplitude and Λ is a diagonal matrix of the squared length-scale hyperparameters.

4. Identification of marine craft

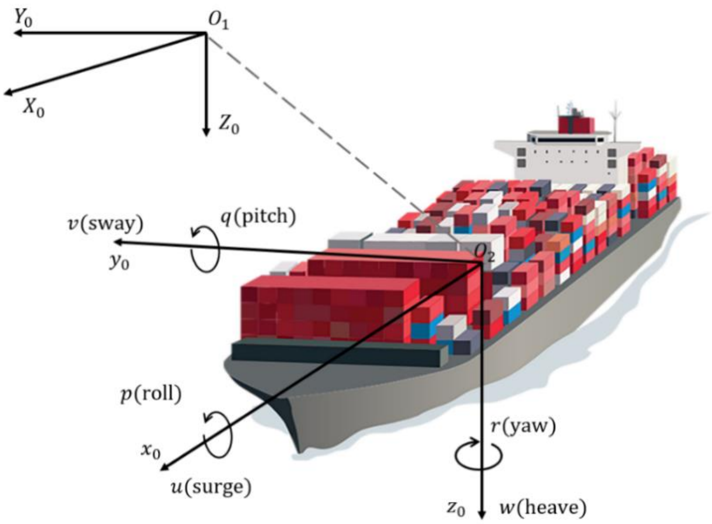

Figure 2. Reference frames for ships

4.1. Parametric gray-box modeling

The essence of the parametric gray-box modeling is to construct a simplified parameterized equation to replace Equation (1). The nondimensional rigid-body kinetics using the Prime system of surface ship 3 DOF maneuvering motion is given as follows:

$$\begin{bmatrix} m' - X'_{\dot{u}} & 0 & 0 \\ 0 & m' - Y'_{\dot{v}} & m'x'_G - Y'_{\dot{r}} \\ 0 & m'x'_G - N'_{\dot{v}} & I'_{zz} - N'_{\dot{r}} \end{bmatrix} \begin{bmatrix} \dot{u}' \\ \dot{v}' \\ \dot{r}' \end{bmatrix} = \begin{bmatrix} F'_1 \\ F'_2 \\ M'_3 \end{bmatrix} \quad (27)$$

where m denotes the ship mass; x_G is the longitudinal coordinate of the ship's center of gravity in the body-fixed coordinate frame; I_z denotes the moments of inertia of the ship about the z_0 axes; $X_{\dot{u}}$, $Y_{\dot{v}}$, $Y_{\dot{r}}$, $N_{\dot{v}}$ and $N_{\dot{r}}$ are acceleration derivatives which can be determined using potential theory; and F_1 F_2 and M_3 are forces and moment disturbing quantity at x_0-axis, y_0-axis and z_0-axis respectively. Note that the superscript " ′ " indicates that the corresponding variable is normalized using the Prime-system.

The selection of a mathematical model for identification is a trade-off between model complexity and model capacity. The most widely used model is the Abkowitz model, a Taylor-series expansion model. The Abkowits model has good generalization performance, but it includes a large number of coefficients and some of the coefficients have no physical meaning. A simplified Abkowitz 3-DOF model [50] is employed to construct the white-box model because it contains fewer hydrodynamic parameters while ensuring high accuracy, which can suppress parameter drift caused by too many variables [51]. The nonlinear forces and moment are defined as:

$$F_1' = X_{hydro} \cdot A(i)$$
$$F_2' = Y_{hydro} \cdot B(i) \quad (28)$$
$$M_3' = N_{hydro} \cdot C(i)$$

where the hydrodynamic derivatives and speed state variables in Equation (28) are as follows:

$X_{hydro} = [X'_u, X'_{vv}, X'_{rr}, X'_{\delta\delta}, X'_{vr}, X'_{v\delta}, X'_{r\delta}, X'_0,]_{1\times 8}$

$Y_{hydro} = [Y'_v, Y'_r, Y'_\delta, Y'_{v|v|}, Y'_{v|r|}, Y'_{|r|r}, Y'_{r|v|}, Y'_{\delta\delta\delta}, Y'_{vv\delta}, Y'_{v\delta\delta}, Y'_{r\delta\delta}, Y'_{rr\delta}, Y'_{rv\delta}, Y'_0]_{1\times 14}$

$N_{hydro} = [N'_v, N'_r, N'_\delta, N'_{v|v|}, N'_{v|r|}, N'_{|r|r}, N'_{r|v|}, N'_{\delta\delta\delta}, N'_{vv\delta}, N'_{v\delta\delta}, N'_{r\delta\delta}, N'_{rr\delta}, N'_{rv\delta}, N'_0]_{1\times 14}$

$A(i) = [u'_a(i), v'^2(i), r'^2(i), \dots, r'(i)\delta'(i) \ ,1 \ ]^T_{1\times 8}$

$B(i) = [v'(i), r'^2(i), \delta'(i), v'(i)|v'(i)|, \dots, r'(i)v'(i)\delta'(i) \ ,1]^T_{1\times 14}$

$C(i) = [v'(i), r'^2(i), \delta'(i), v'(i)|v'(i)|, \dots, r'(i)v'(i)\delta'(i) \ ,1]^T_{1\times 14}$

where the relative speed $u_a = u - u_{nom}$. As seen, there is a total of 36 hydrodynamic parameters in the simplified Abkowitz model. Euler's stepping method is utilized to discretize the equation of motions. The constructor of samples for hydrodynamic parameter estimation can be obtained as follows:

Input variables: $[A(i), B(i), C(i)]$

Output response:

$$\begin{bmatrix} (m' - X'_{\dot{u}})L\dfrac{u_a'(i+1) - u_a'(i)}{U(i)\,\triangle t} \\ (m' - Y'_{\dot{v}})L\dfrac{v'(i+1) - v'(i)}{U(i)\,\triangle t} + (m'x'_G - Y'_{\dot{r}})L\dfrac{r'(i+1) - r'(i)}{U(i)\,\triangle t} \\ (m'x'_G - N_{\dot{v}})L\dfrac{v'(i+1) - v'(i)}{U(i)\,\triangle t} + (I'_{zz} - N_{\dot{r}})L\dfrac{r'(i+1) - r'(i)}{U(i)\,\triangle t} \end{bmatrix} \quad (29)$$

where $U = \sqrt{u^2 + v^2}$ is the resultant speed in the horizontal plane and $\triangle t$ is the time sample.

The procedure of the parametric gray-box modeling and motion prediction using ScBR is briefly depicted in Fig. 3. A Bayesian optimization algorithm (BOA) is employed to tune the value of prior variance, V, in semi-conjugate regression. For more details regarding the use of semi-conjugate regression with BOA to identify the parameters, please refer to our previous work [40].

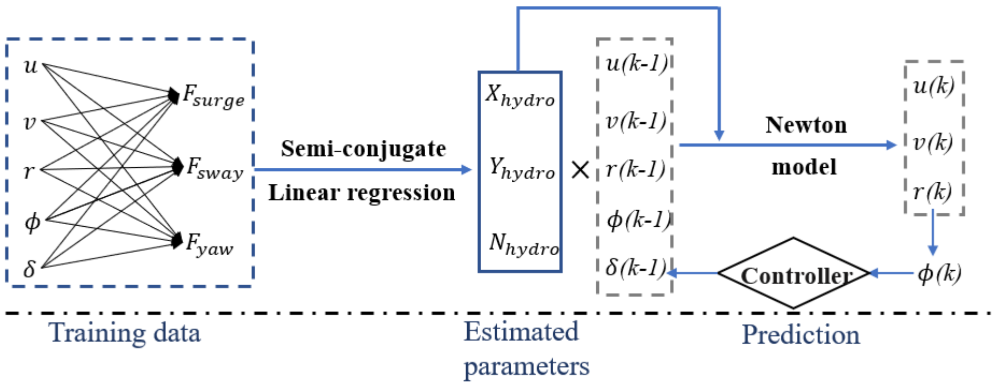

Figure 3. Process of parametric gray-box modeling using ScBR

4.2. Black-box modeling

A continuous-time black-box model directly describes the relationship between the input variables and out response without any constrains. The principal parameters and the mathematical model are not required in the black-box modeling. The structure of the training data follows the form

Input variables: $[u(i-1), v(i-1), r(i-1), \delta(i-1)]$

Output response: $[u(i), v(i), r(i)]$ (30)

Preprints (www.preprints.org) | NOT PEER-REVIEWED | Posted: 16 September 2020 doi:10.20944/preprints202009.0365.v1

Fig. 4 shows the process of black-box modeling and motion prediction using NIGP. The SVM is also used with the same training data for comparison with Bayesian regression. The RBF kernel function in Equation (31), with an automatic kernel scale σ_{SVM}, is used to train the SVM.

$$k\left(x_i, x_j\right) = \exp\left(-\frac{\left|x_i - x_j\right|^2}{2\sigma_{SVM}}\right) \tag{31}$$

BOA is employed to tune the hyperparameters in SVM using the 'Bayesopt' MATLAB function. In theory, this scheme can overcome the drawbacks of parametric gray-box models, such as a failure to represent the actual behavior of the system due to unmodeled components.

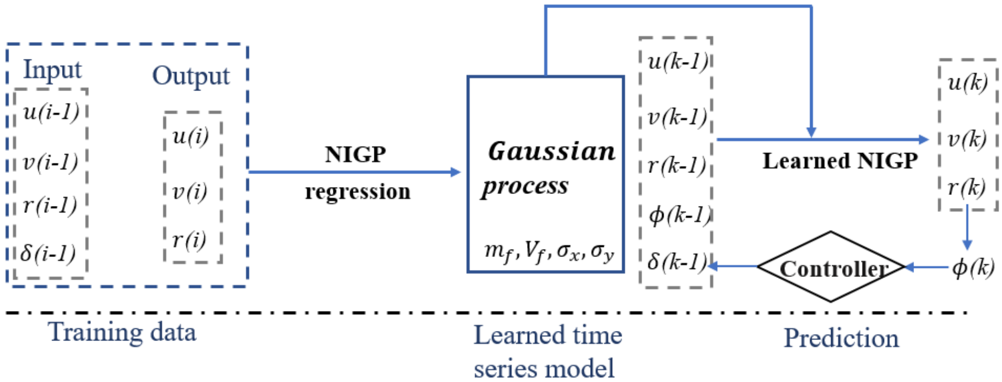

Figure 4. Process of black-box modeling using NIGP

4.3. A case study of a large container ship

The ship used in the experimental tests is a scale model of large tankers, KVLCC2, one of the benchmark ships for verification and validation of ship maneuvering simulation methods recommended by Simulation Workshop for Ship Maneuvering (SIMMAN) [52]. Maneuvering and course maintaining tests with the KVLCC2 models have been performed at the Hamburg Ship Model Basin (HSVA). The dimensions of the vessel and the scale model are detailed in Table 2.

Table 2. Particulars of KVLCC2

Elements	Full-scale	model
L_{pp} (m)	320.0	7.0
B (m)	58.0	1.1688
D (m)	30.0	0.6563
Displacement (m^3)	312622	3.2724
Draught (m)	20.8	0.4550
Beam coefficient	0.8098	0.8098
Nominal speed (m/s)	7.97	1.18
Rudder speed ($\dot{\delta}$)	2.3 deg/s	15.8 deg/s
Nondim mass (m')	1908×10^{-5}	
Nondim x coordinate of CG(x'_G)	3486×10^{-5}	
Nondim inertia in yaw (I'_z)	119×10^{-5}	

Here, 35°/5° zigzag maneuver data with a cumulative time of 180 s is used for training the parametric gray-box model using ScBR, and the sample time is 0.5 s. The hyperparameters of ScBR, prior variance V, are tuned by BOA. The posterior hydrodynamic parameters estimated by ScBR are listed in Table 3. The added mass, including $X'_{\dot{u}}$ and $Y'_{\dot{v}}$, is calculated by slender-body instead of SI [53]. For comparison of the ScBR, Luo and Li's results of SVM under the same parameterization gray-box modeling are also listed in the table. It should be noted that the mainstream algorithms for marine equipment identification are offline algorithms, which is usually trained after the data are obtained and then deployed in the controller or simulation system [10]. Therefore, the time spent on tuning the hyperparameters will not be mentioned in the article.

Table 3. The nondimensional hydrodynamic parameters for ScBR and SVM (1×10^{-5})

X-Coef.	ScBR	SVM	Y-Coef.	ScBR	SVM	N-Coef.	ScBR	SVM
X'_u	-140.1	-128	Y'_v	350.4	-94	N'_v	-44.8	-54.9
X'_{vv}	152.6	175	Y'_r	1936.0	2066	N'_r	-125.5	-82.9
X'_{rr}	-180.0	-118	Y'_δ	568.3	486	N'_δ	-180.9	-146.8
$X'_{\delta\delta}$	125.2	-116	$Y'_{v\|v\|}$	68.7	63	$N'_{v\|v\|}$	5.4	-5.4
X'_{vr}	-328.2	-303	$Y'_{v\|r\|}$	128.5	67	$N'_{v\|r\|}$	-3.3	2.6
$X'_{v\delta}$	245.2	196	$Y'_{\|r\|r}$	932.6	737	$N'_{\|r\|r}$	-48.5	-30.8
$X'_{r\delta}$	-584.2	-455	$Y'_{r\|v\|}$	30.8	177	$N'_{r\|v\|}$	-14.3	-5.5
X'_0	-144.0	-85	$Y'_{\delta\delta\delta}$	216.3	-58	$N'_{\delta\delta\delta}$	-65.2	-52.9
			$Y'_{vv\delta}$	98.7	29	$N'_{vv\delta}$	-9.6	-8.0
			$Y'_{v\delta\delta}$	41.0	17	$N'_{v\delta\delta}$	1.6	-6.3
			$Y'_{r\delta\delta}$	306.5	-50	$N'_{r\delta\delta}$	9.6	6.1
			$Y'_{rr\delta}$	314.2	99	$N'_{rr\delta}$	12.4	12.9
			$Y'_{rv\delta}$	350.4	-40	$N'_{rv\delta}$	-44.8	2.1
			Y'_0	1936.0	-56	N'_0	-125.5	1.4
Added mass	$X'_{\dot{u}}$	−95.4	$Y'_{\dot{v}}$	−1283			$N'_{\dot{v}}$	0
not identified			$Y'_{\dot{r}}$	0			$N'_{\dot{r}}$	-107

Here, 35°/5° and 20/5° zigzag maneuvers every 5 s are used for training the black-box modeling driven by NIGP and SVM. It is of no application value to predict the training movement of ship by using the model obtained from the training data. To verify the generalization ability of the models identified by gray-box modeling and black-box modeling driven by SVM and Bayesian regression, the 30°/5° and 15°/5° zigzag tests are predicted. Fig. 5 and Fig. 6 show the prediction results of each method, and the root mean square error (RMSE) is adopted to analyze the prediction performance of these methods, which is shown in Table 4. In addition, the computation time of each step of these methods for prediction is also listed in the table. From the validation results, it can be concluded that the trends of all the predictions before 70 s are basically consistent with the experiment. After 70 s, the difference between the predictions results of various methods gradually increased. On the whole, the parametric gray-box and black-box modeling based on Bayesian regression results are in acceptable agreement with the validation samples and show a stronger ability to predict than SVM. From the perspective of the modeling framework, the prediction results of gray-box modeling are better than those of black-box modeling in 30°/5° zigzag maneuvers, but worse in 15°/5° zigzag tests. The main reason is that the training data of gray-box modeling only contains 35°/5° movement, which is closer to the 30°/5° zigzag validation test. For the prediction time, parametric gray-box modeling is significantly faster than black-box modeling because the calculation process of parametric gray-box modeling is entirely linear. Because it considers the input noise and variance in the calculation process, NIGP spends more time on the prediction than SVM. Note that the black-box modeling usually requires more training data to enhance generalization ability than parametric gray-box modeling, because the specified framework of the parametric gray-box model already contains some information about the system. In a similar study [24], four groups of ship maneuver datasets are used for training black-box models while one group dataset is used for parameter estimation.

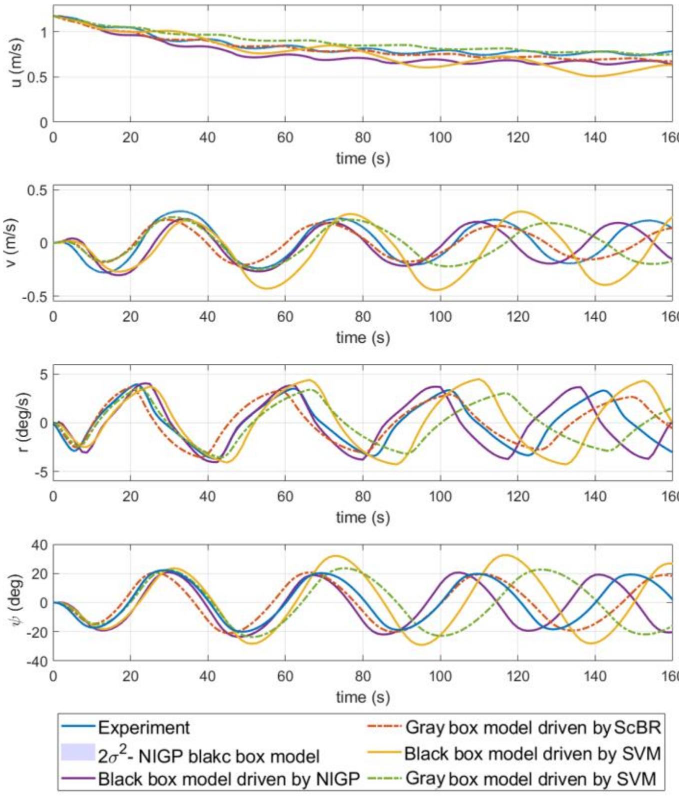

Figure 5. Comparisons of results of the ship predicted motion; the 30°/5° zigzag test

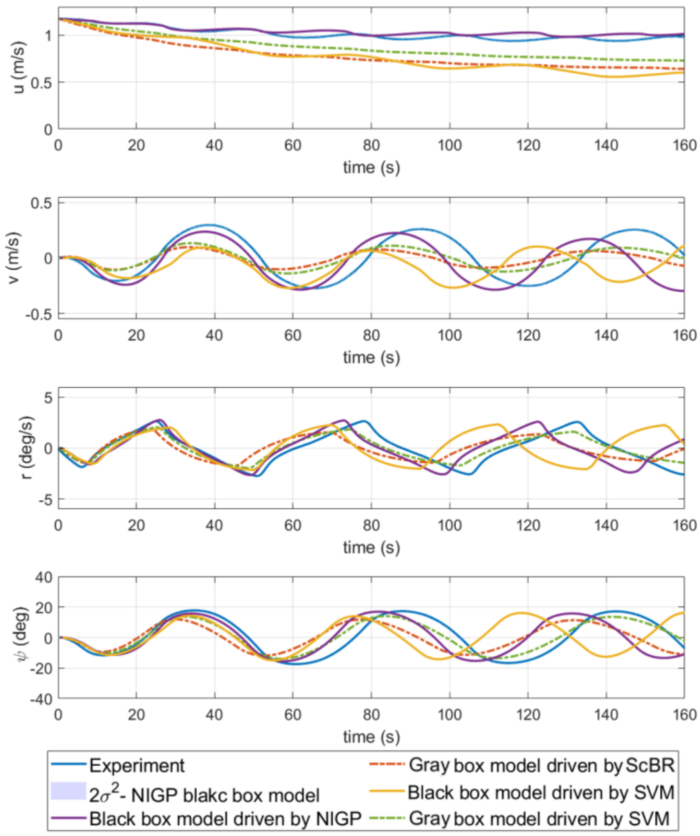

Figure 6. Comparisons of results of the ship predicted motion; the 15°/5° zigzag test

Preprints (www.preprints.org) | NOT PEER-REVIEWED | Posted: 16 September 2020 doi:10.20944/preprints202009.0365.v1

Table 4. Estimation of forecast accuracy by RMSE and computation time for the validation test

		Parametric gray-box model		Black-box model	
		SVM	ScBR	SVM	NIGP
30°/5°	u	0.053	0.040	0.115	0.094
	v	0.182	0.092	0.186	0.121
	r	2.530	1.226	2.213	1.834
15°/5°	u	0.155	0.240	0.262	0.021
	v	0.126	0.163	0.238	0.062
	r	0.605	1.294	2.140	0.443
time (s/step)		0.0009		0.004	0.014

5. Identification of WEC

5.1. Nonparametric gray-box modeling

Similar to the ship model in Equation (27), the time domain 3 DOF model of the WEC buoy is given as,

$$\begin{bmatrix} m - X'_{\dot{u}} & 0 & 0 \\ 0 & m' - Z'_{\dot{w}} & m' y'_G - Z'_{\dot{q}} \\ m z_G & -m x_G & I_{zz} \end{bmatrix} \begin{bmatrix} \dot{u} \\ \dot{w} \\ \dot{q} \end{bmatrix} = \begin{bmatrix} F'_1 \\ F'_3 \\ M'_2 \end{bmatrix} \tag{32}$$

Different from the parametric model in Equation (28), the force and moment on the right side of the equation are not fitted by the method of multiplying the hydrodynamic coefficient and the speed. In this case, NIGP is adopted to perform nonlinear regression between forces, speed and other variables. The training sample that couples hydrodynamic forces and moment nonlinear regression for training NIGP is

Input variables: $[u(i), w(i), q(i), h(i)]$

Output response:

$$\begin{bmatrix} (m - X_{\dot{u}}) \dfrac{u(i+1) - u(i)}{\Delta t} \\ (m - Z_{\dot{w}}) \dfrac{w(i+1) - w(i)}{\Delta t} + (m y_G - Z_{\dot{q}}) \dfrac{q(i+1) - q(i)}{\Delta t} \\ m z_G \dfrac{u(i+1) - u(i)}{\Delta t} - m x_G \dfrac{w(i+1) - w(i)}{\Delta t} + I_{zz} \dfrac{q(i+1) - q(i)}{\Delta t} \end{bmatrix} \tag{33}$$

The process of nonparametric gray-box modeling and motion prediction using NIGP is depicted in Fig. 7.

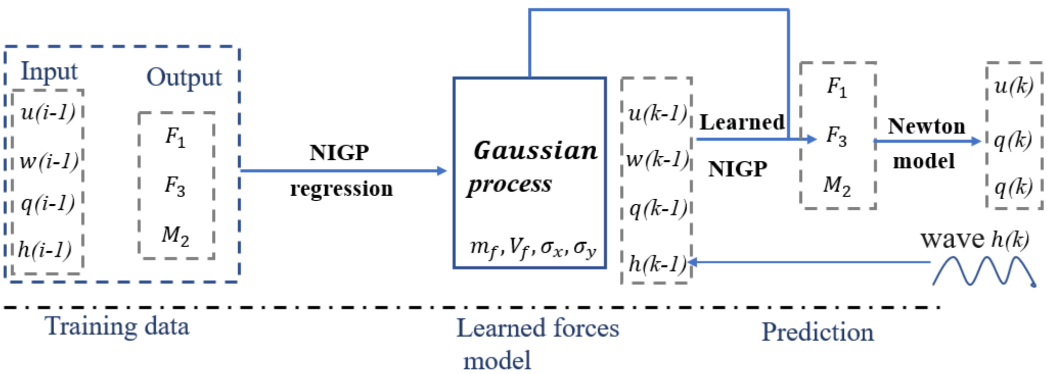

Figure 7. Process of nonparametric gray-box modeling of the WEC using NIGP

5.2. Black-box modeling

In the same way as the black-box modeling of the ship, only the time series of motion state variables and wave height are used to train the NIGP model. The structure of the training data follows the form

Input variables: $[u(i-1), w(i-1), q(i-1), h(i-1)]$

Output response: $[u(i), w(i), q(i)]$ (34)

The detailed process of the black-box modeling of the WEC using NIGP is shown in Fig. 8.

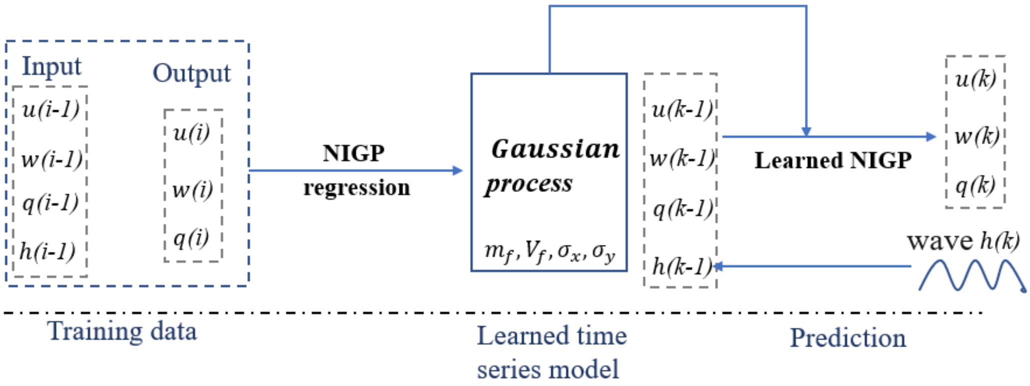

Figure 8. Process of black-box modeling of the WEC using NIGP

5.3. A case study of a multi-freedom buoy WEC

The experiment was carried out in the wave tank of Shandong Provincial Key Laboratory of Ocean Engineering [54], shown in Fig. 9. The model had 3 DOFs: surge, heave and pitch. Every DOF was independent and could be fixed. The buoy's motion was measured by an NDI Optotrak Certus 3D investigator. The sliding frame of surge was 58 kg. A spring was used in surge to provide the restoring force. The added mass can be calculated as

$$m_\infty = A(\omega) + \frac{1}{\omega}\int_0^\infty K(t)\, sin(\omega t)\, dt$$
$$K(t) = \frac{2}{\pi}\int_0^\infty B(\omega)\, cos(\omega t)\, dt \tag{35}$$

where ω is the wave frequency and $\boldsymbol{B}(\omega)$ is the radiation damping matrix. The values of $\boldsymbol{A}(\omega)$ and $\boldsymbol{B}(\omega)$ are calculated by the ANSYS AQWA software package (AQWA-LINE suite), which implements a boundary element method algorithm.

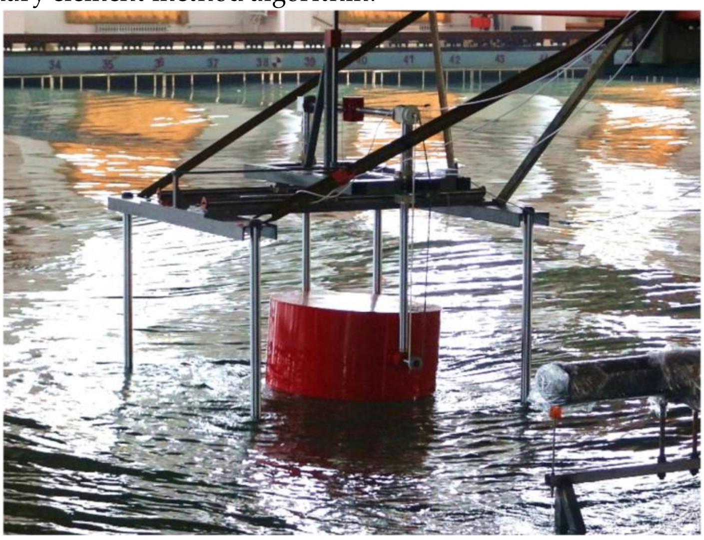

Figure 9. Physical model experiment

Preprints (www.preprints.org) | NOT PEER-REVIEWED | Posted: 16 September 2020 doi:10.20944/preprints202009.0365.v1

Table 5. Particulars and test conditions of the WEC

Elements	Value
Water depth (m)	1.0
Wave heihgt (m)	0.2
Radius (m)	0.4
Draft (m)	0.4
Height (m)	0.12
Spring stiffness coefficient	85 N/m
Mass (kg)	58
Inertia in yaw (I_{zz})	2.2

The wave period of the experimental data is 1.6 s. The first 30 s of the experimental data are used to train each model, and the last 15 seconds of the data are used as the test set to verify the accuracy of the identified models. The sampling interval of training data for nonparametric gray-box modeling is 0.05 s, while the black-box modeling is 0.1 s. It can be seen from Fig. 10 that, except for the nonparametric gray-box model driven by SVM, the predicted results of the other three methods are almost the same as the experimental values. The rest motion data with a wave period of 1.8 s is used to further verify the identified models and is presented in Fig. 11. It should be noted that the WEC buoy has different added mass in a different wave frequency, so we recalculated the added mass with the wave period 1.8 s and substituted it in Equation (31) for gray-box modeling prediction. From Fig. 11, it can be seen that the trend of the experimental and Bayesian gray-box and black-box modeling prediction fit well in the motion of surge and heave. However, it can be observed that there is some discrepancy between the prediction and the experiment in pitch. This may be mainly due to fact that the frequency of wave in the training data is higher than that of the test, and the motion is very regular, which means that the training data does not fully reflect the dynamic characteristics of the device. In the 1.8 s wave period, the prediction of the gray-box modeling based on SVM failed, and its motion state was significantly slower than the experiment. The RMSE of u, w and q and computation time of the models are listed in Table 6. Table 6 demonstrates that the black-box model based on NIGP is the most accurate identification method for WEC buoy.

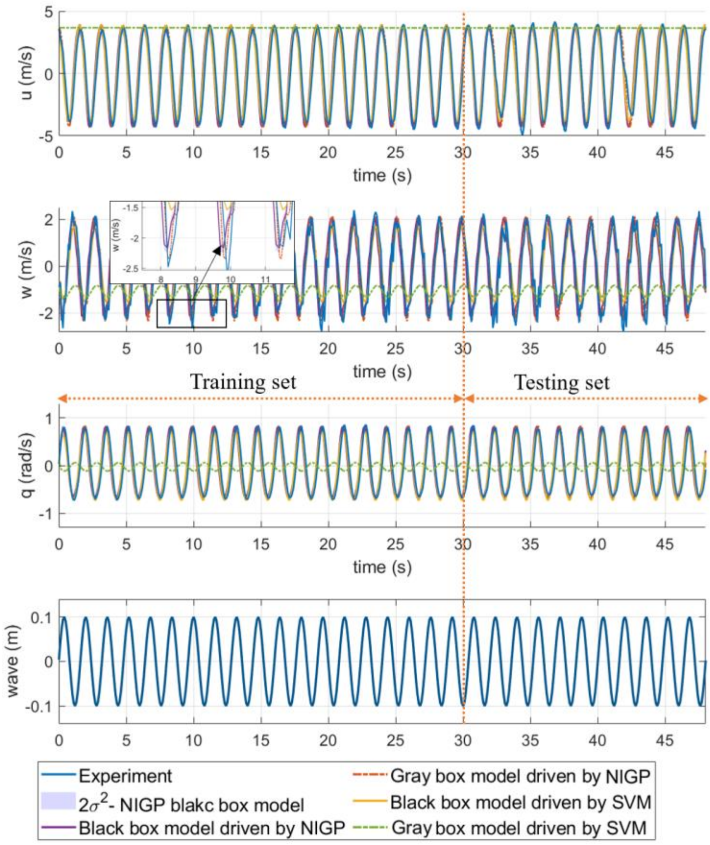

Figure 10. Comparisons of results of the WEC predicted motion; T=1.6 s

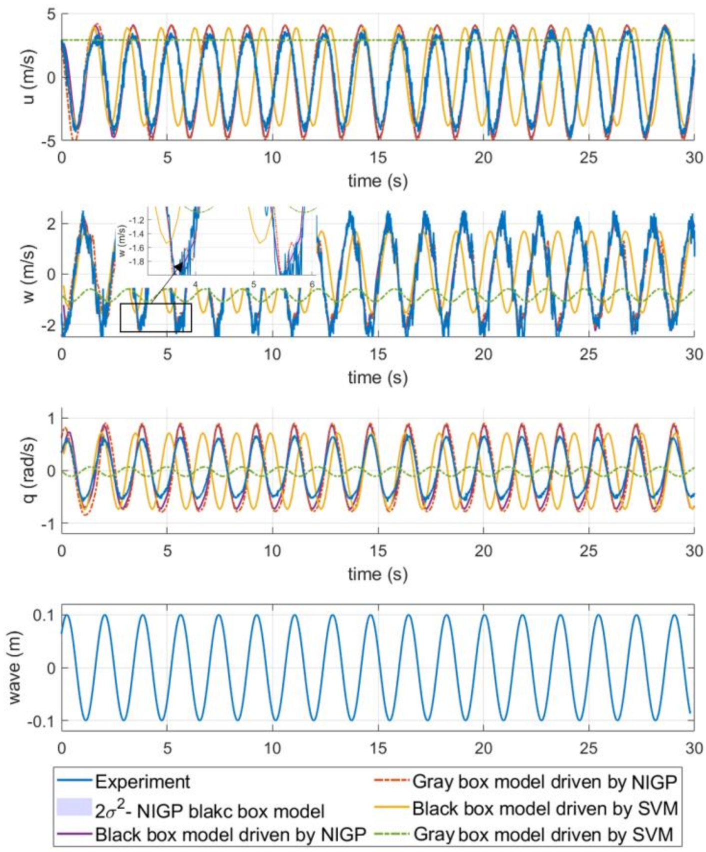

Figure 11. Comparisons of results of the WEC predicted motion; T=1.8 s

Preprints (www.preprints.org) | NOT PEER-REVIEWED | Posted: 16 September 2020 doi:10.20944/preprints202009.0365.v1

Table 6. Estimation of forecast accuracy by RMSE and computation time for the WEC motion with the wave period 1.6 s and 1.8 s

		Nonparametric gray-box model		**Black-box model**	
		SVM	NIGP	SVM	NIGP
T=1.6 s	*u*	/	0.866	1.883	2.184
	w	/	0.580	0.610	1.143
	q	/	0.151	0.346	0.404
T=1.8 s	*u*	/	1.503	3.872	1.142
	w	/	0.979	1.935	0.620
	q	/	0.396	0.664	0.211
time (s/step)		0.0012	0.086	0.0013	0.025

6. Discussions and Conclusions

In this work, three different identification frameworks, parametric gray-box modeling, nonparametric gray-box modeling and black-box modeling based on Bayesian regression, have been developed. The main objective is to propose a robust and widely used identification methodology for hydrodynamic models of marine vehicles and equipment using experimental data. The Bayesian regression approach was compared with SVM on a KVLCC2 and WEC buoy model and showed good generalization ability. The relative strengths and weakness of each method are summarized in Table 7. For different modeling objects and characteristics, the corresponding modeling method should be selected according to their capabilities. For conversional ship, choosing traditional parametric modeling can produce good results under the limited data conditions. For new types of vehicles such as USV and ROV, as well as other irregularly shaped marine structures, nonparametric modeling could be a better choice. However, when very low amounts of training data exist, the parametric gray-box modeling method can provide a useful model with the help of prior knowledge such as the added mass of the marine equipment. The obtained experimental data is usually the velocity obtained by MRU (motion reference unit) or displacement data measured with a camera. If the force of the device can be obtained by CFD simulation, or directly measured by a PMM test, the nonparametric gray-box modeling with nonlinear fluid dynamics would be a very effective method. In terms of the practicality of the algorithm, compared with SVM and ANN, Bayesian regression introduces a prior into the loss function, which has stronger generalization ability. Moreover, NIGP shows stronger predictive ability because of its additional processing of input noise. However, it needs to be acknowledged that it costs longer execution time due to the complicated calculations in nonparametric modeling.

Table 7. Capabilities and challenges of Bayesian gray-box modeling and black-box modeling

Property	**Parametric gray-box model driven by ScBR**	**Nonparametric gray-box driven by NIGP**	**Black-box model driven by NIGP**
Modeling framework	Newton's second law equation with Taylor expansion forces	Newton's second law equation with nonparametric forces	High-dimensional mapping of time series
Required prior knowledge	weak	fair	strong
Nonlinearities	fair	strong	strong
Training with limited data	strong	fair	weak
Noise robustness	weak	fair	strong
Execution time	strong	weak	fair

Although the preliminary application of the proposed Bayesian methods seems encouraging thus far, the work needs further extension and investigations. (1) For a model calculation to be used in the practical application of control design, the training dataset should be richer and obtained from more abundant excitation signal, to make the identification model more accurate. The experimental data used in this article are not from the experiments specially designed for system identification, so the excitation signal of the training data is not enough. Especially for the wave energy device, compared with regular waves, the motion data under irregular waves (such as Jonswap spectral waves) can better reflect the dynamic characteristics of the device. (2) The experiments of ship and WEC in this article are all carried out in water tank, but the equipment in the ocean will be affected by various factors such as wind, water depth and current. Further study is required to introduce these factors as inputs into nonparametric modeling. (3) Model predictive control (MPC) based on GP allows the direct assessment of residual model uncertainly to enable cautious control. It is very interesting to integrate NIGP-based nonlinear nonparametric modeling into MPC for marine systems.

Author Contributions: Conceptualization, Y.L. and Y.X.; methodology, Y.X and G.X.; software, Y.X. and S.H; validation, Y.X., S.H. and Q.J.; resources, Y.L.; data curation, S.H. and Q.J.; writing and editing, Y.X. and G.X. All authors have read and agreed to the published version of the manuscript.

Funding: This research was funded by National Key R&D Program of China, grant number 2019YFB2005303; Shandong Provincial Key Research and Development Program Major Scientific and Technological Innovation Project under Grant 2019JZZY010802; the Laboratory for Marine Geology, Qingdao National Laboratory for Marine Science and Technology, grant number MGQNLM201806.

Acknowledgments: The authors would like to thank the Qingdao Postdoctoral Applied Research Project (Hydrodynamic characteristic and power performance of multi-freedom buoy wave energy converter); the Hamburg Ship Model Basin (HVSA) and SIMMAN for sharing the KVLCC2 experimental data, and the Ocean University of China for their technical support for the experiment of the WEC.

Conflicts of Interest: The authors declare no conflict of interest.

References

1. IMO. Regulatory Scoping Exercise for the Use of Maritime Autonomous Surface Ships (MASS) Report of the Working Group. In Proceedings of MSC 99th Session, London, Aug.
2. Pena-Sanchez, Y.; Windt, C.; Davidson, J.; Ringwood, J.V. A Critical Comparison of Excitation Force Estimators for Wave-Energy Devices. *IEEE Transactions on Control Systems Technology* 2019, 10.1109/tcst.2019.2939092, 1-13, doi:10.1109/tcst.2019.2939092.
3. Ljung, L. Black-box models from input-output measurements. In Proceedings of IEEE Instrumentation & Measurement Technology Conference.
4. Drazin, P.G.; Reid, W.H. *Hydrodynamic stability*; Cambridge university press: 2004.
5. Norrbin, N.H. *Theory and observations on the use of a mathematical model for ship manoeuvring in deep and confined waters*; Swedish State Shipbuilding Experimental Tank Goteborg: 1971.
6. Abkowitz, M. Lectures on ship hydrodynamics. *Hydro-Og Aerodynamisk Laboratorium, Report Hy-5* 1964.
7. Kobayashi, E.; Kagemoto, H.; Furukawa, Y. Research on ship manoeuvrability and its application to ship design. Chapter 2: mathematical models of manoeuvring motions. In Proceedings of The 12th Marine Dynamic Symposium; pp. 23-90.
8. Astrom, K. Design of fixed gain and adaptive autopilots based on the Nomoto model. In Proceedings of Proceedings, Symposium on Ship Steering Automatic Control.
9. Furukawa, Y.; Delefortrie, G.; Duffy, J.; Guillerm, P.; Kim, S.; Mauro, S.; Otzen, J.; Simonsen, C.; Steinwand, M.; Tannuri, E. Final Report and recommendations of the Manoeuvring Committee. In Proceedings of The 28th International Towing Tank Conference (ITTC); pp. 131-212.
10. Sutulo, S.; Guedes Soares, C. An algorithm for offline identification of ship manoeuvring mathematical models from free-running tests. Ocean Engineering 2014, 79, 10-25, doi:10.1016/j.oceaneng.2014.01.007.
11. Pintelon, R.; Schoukens, J. System Identification: A Frequency Domain Approach, Second Edition; IEEE Press: 2012.

12. Nagumo, J.; Noda, A. A learning method for system identification. Journal of the Society of Instrument Control Engineers 1967, 12, 282-287.
13. Fossen, T.I.; Sagatun, S.I.; Sørensen, A.J. Identification of Dynamically Positioned Ships. Ifac Proceedings Volumes 1995, 28, 362-369.
14. Åström, K.J.; Källström, C.G. Identification of Ship Steering Dynamics. Journal of Ningbo Univeristy 1989.
15. Mei, B.; Sun, L.; Shi, G. White-Black-Box Hybrid Model Identification Based on RM-RF for Ship Maneuvering. IEEE Access 2019, 7, 57691-57705, doi:10.1109/access.2019.2914120.
16. Wang, Z.; Zou, Z.; Guedes Soares, C. Identification of ship manoeuvring motion based on nu-support vector machine. Ocean Engineering 2019, 183, 270-281, doi:10.1016/j.oceaneng.2019.04.085.
17. Cummins, W. The impulse response function and ship motions; David Taylor Model Basin Washington DC: 1962.
18. Li, Y.; Yu, Y.-H. A synthesis of numerical methods for modeling wave energy converter-point absorbers. Renewable and Sustainable Energy Reviews 2012, 16, 4352-4364.
19. Davidson, J.; Giorgi, S.; Ringwood, J.V. Identification of Wave Energy Device Models From Numerical Wave Tank Data—Part 1: Numerical Wave Tank Identification Tests. IEEE Transactions on Sustainable Energy 2016, 7, 1012-1019, doi:10.1109/tste.2016.2515512.
20. Nguyen, H.N.; Tona, P. Wave Excitation Force Estimation for Wave Energy Converters of the Point-Absorber Type. IEEE Transactions on Control Systems Technology 2017, PP, 1-9.
21. Davis, A.F.; Fabien, B.C. Systematic identification of drag coefficients for a heaving wave follower. Ocean Engineering 2018, 168, 1-11, doi:10.1016/j.oceaneng.2018.08.054.
22. Perez, T.; Fossen, T.I. A Matlab Toolbox for Parametric Identification of Radiation-Force Models of Ships and Offshore Structures. Modeling, Identification and Control: A Norwegian Research Bulletin 2009, 30, 1-15, doi:10.4173/mic.2009.1.1.
23. Garcia-Abril, M.; Paparella, F.; Ringwood, J.V. Excitation force estimation and forecasting for wave energy applications. IFAC-PapersOnLine 2017, 50, 14692-14697.
24. Wang, X.-g.; Zou, Z.-j.; Yu, L.; Cai, W. System identification modeling of ship manoeuvring motion in 4 degrees of freedom based on support vector machines. China Ocean Engineering 2015, 29, 519-534, doi:10.1007/s13344-015-0036-9.
25. Xu, H.; Guedes Soares, C. Manoeuvring modelling of a containership in shallow water based on optimal truncated nonlinear kernel-based least square support vector machine and quantum-inspired evolutionary algorithm. Ocean Engineering 2020, 195, doi:10.1016/j.oceaneng.2019.106676.
26. Shi, S.; Abdelrahman, M.; Patton, R.J.; Ieee. Wave Excitation Force Estimation and Forecasting for WEC Power Conversion Maximisation. In 2019 Ieee/Asme International Conference on Advanced Intelligent Mechatronics, Ieee: New York, 2019; pp. 526-531.
27. Rajesh, G.; Bhattacharyya, S.K. System identification for nonlinear maneuvering of large tankers using artificial neural network. Applied Ocean Research 2008, 30, 256-263, doi:10.1016/j.apor.2008.10.003.
28. Wang, N.; Er, M.J.; Han, M. Large Tanker Motion Model Identification Using Generalized Ellipsoidal Basis Function-Based Fuzzy Neural Networks. IEEE Trans Cybern 2015, 45, 2732-2743, doi:10.1109/TCYB.2014.2382679.
29. Nagulan, S.; Selvaraj, J.; Arunachalam, A.; Sivanandam, K. Performance of artificial neural network in prediction of heave displacement for non-buoyant type wave energy converter. IET Renewable Power Generation 2017, 11, 81-84, doi:10.1049/iet-rpg.2015.0416.
30. Desouky, M.A.A.; Abdelkhalik, O. Wave prediction using wave rider position measurements and NARX network in wave energy conversion. Applied Ocean Research 2019, 82, 10-21, doi:10.1016/j.apor.2018.10.016.
31. Vapnik, V.N. The Nature of Statistical Learning Theory; Springer: 2000.
32. Ariza Ramirez, W.; Leong, Z.Q.; Nguyen, H.; Jayasinghe, S.G. Non-parametric dynamic system identification of ships using multi-output Gaussian Processes. Ocean Engineering 2018, 166, 26-36, doi:10.1016/j.oceaneng.2018.07.056.
33. Bai, W.; Ren, J.; Li, T. Modified genetic optimization-based locally weighted learning identification modeling of ship maneuvering with full scale trial. Future Generation Computer Systems 2019, 93, 1036-1045, doi:10.1016/j.future.2018.04.021.

34. Moreno-Salinas, D.; Moreno, R.; Pereira, A.; Aranda, J.; de la Cruz, J.M. Modelling of a surface marine vehicle with kernel ridge regression confidence machine. Applied Soft Computing 2019, 76, 237-250, doi:10.1016/j.asoc.2018.12.002.
35. Petra, N.; Petra, C.G.; Zhang, Z.; Constantinescu, E.M.; Anitescu, M. A Bayesian Approach for Parameter Estimation With Uncertainty for Dynamic Power Systems. IEEE Transactions on Power Systems 2017, 32, 2735-2743, doi:10.1109/tpwrs.2016.2625277.
36. Mattos, C.L.C.; Barreto, G.A. A stochastic variational framework for Recurrent Gaussian Processes models. Neural Netw 2019, 112, 54-72, doi:10.1016/j.neunet.2019.01.005.
37. Bin-Karim, S.; Bafandeh, A.; Baheri, A.; Vermillion, C. Spatiotemporal Optimization Through Gaussian Process-Based Model Predictive Control: A Case Study in Airborne Wind Energy. IEEE Transactions on Control Systems Technology 2019, 27, 798-805, doi:10.1109/tcst.2017.2779428.
38. Kruschke, J.K. Doing Bayesian Data Analysis. Wiley Interdisciplinary Reviews Cognitive Science 2010, 1, 658-676.
39. Kocijan, J. Modelling and control of dynamic systems using Gaussian process models; Springer: 2016.
40. Xue, Y.; Liu, Y.; Ji, C.; Xue, G. Hydrodynamic parameter identification for ship manoeuvring mathematical models using a Bayesian approach. Ocean Engineering 2020, 195, doi:10.1016/j.oceaneng.2019.106612.
41. Astfalck, L.C.; Cripps, E.J.; Hodkiewicz, M.R.; Milne, I.A. A Bayesian approach to the quantification of extremal responses in simulated dynamic structures. Ocean Engineering 2019, 182, 594-607, doi:10.1016/j.oceaneng.2019.04.035.
42. Fossen, T.I. Handbook of Marine Craft Hydrodynamics and Motion Control; 2011.
43. Robert; Christian. Machine learning, a probabilistic perspective; Taylor & Francis: 2014.
44. Murphy, K.P. Machine learning: a probabilistic perspective; MIT press: 2012.
45. Gelfand, A.E.; Smith, A.F. Sampling-based approaches to calculating marginal densities. Journal of the American statistical association 1990, 85, 398-409.
46. Bull, A.D. Convergence rates of efficient global optimization algorithms. Journal of Machine Learning Research 2011, 12, 2879-2904.
47. Mchutchon, A.; Rasmussen, C.E. Gaussian Process Training with Input Noise. In Proceedings of neural information processing systems; pp. 1341-1349.
48. McHutchon, A.J. Nonlinear modelling and control using Gaussian processes. University of Cambridge, 2015.
49. Bijl, H. LQG and Gaussian process techniques: For fixed-structure wind turbine control. Delft University of Technology, 2018.
50. Luo, W.; Guedes Soares, C.; Zou, Z. Parameter Identification of Ship Maneuvering Model Based on Support Vector Machines and Particle Swarm Optimization. Journal of Offshore Mechanics and Arctic Engineering 2016, 138, doi:10.1115/1.4032892.
51. Wang, Z.-H.; Zou, Z.-J. Quantifying Multicollinearity in Ship Manoeuvring Modeling by Variance Inflation Factor. In Proceedings of ASME 2018 37th International Conference on Ocean, Offshore and Arctic Engineering.
52. Simonsen, C.; Stern, F. SIMMAN 2014 workshop on verification and validation of ship maneuvering simulation methods. In Proceedings of Draft Workshop Proceedings.
53. Luo, W.; Li, X. Measures to diminish the parameter drift in the modeling of ship manoeuvring using system identification. Applied Ocean Research 2017, 67, 9-20, doi:10.1016/j.apor.2017.06.008.
54. Huang, S.-t.; Shi, H.-d.; Dong, X.-c. Capture Performance of A Multi-Freedom Wave Energy Converter with Different Power Take-off Systems. China Ocean Engineering 2019, 33, 288-296, doi:10.1007/s13344-019-0028-2.